# Network of inherent structures in spin glasses: Scaling and scale-free distributions

Z. Burda
*Marian Smoluchowski Institute of Physics and Mark Kac Complex Systems Research Centre, Jagellonian University, Reymonta 4, 30-059 Krakow, Poland*

A. Krzywicki
*Laboratoire de Physique Théorique, Bâtiment 210, Université Paris-Sud, F-91405 Orsay, France*

O. C. Martin
*Université Paris-Sud, UMR8626, LPTMS, Orsay, F-91405 France*
*and CNRS, Orsay, F-91405, France*

(Received 16 July 2007; published 9 November 2007)

The local minima (inherent structures) of a system and their associated transition links give rise to a network. Here we consider the topological and distance properties of such a network in the context of spin glasses. We use steepest descent dynamics, determining for each disorder sample the transition links appearing within a given barrier height. We find that differences between linked inherent structures are typically associated with local clusters of spins; we interpret this within a framework based on droplets in which the characteristic "length scale" grows with the barrier height. We also consider the network connectivity and the degrees of its nodes. Interestingly, for spin glasses based on random graphs, the degree distribution of the network of inherent structures exhibits a nontrivial scale-free tail.

DOI: 10.1103/PhysRevE.76.051107 PACS number(s): 05.50.+q, 75.10.Nr, 75.40.Mg, 89.75.Fb

## I. INTRODUCTION

In typical complex systems, there is a huge number of inherent structures [1] (local minima of energy in the configuration space), with no single one giving a good approximation to the equilibrium state. Indeed, it is necessary to consider most if not all inherent structures and their basins to reach a quantitative understanding of a model's equilibrium properties [2,3]. To include also the dynamics, it is necessary to know how these basins are connected (linked) by saddles, the (excitation) energies of which play an important role for the associated transition rates [4–10]. The set of local minima and their links define a network [11,12]; following Doye [12], we shall refer to it as the "Inherent Structure Network" or "ISN." Such a framework has been applied to water [6], atomic clusters [12], and glasses [11]; all these systems have a somewhat complex energy landscape but none has quenched disorder.

In this work, we focus on the inherent structure network (ISN) in the context of spin glasses [13] because they combine quenched disorder and complex energy landscapes; in addition, their landscapes are based on microscopic Hamiltonians rather than on an abstract random potential [14,15]. Of particular interest are the network's topology, how the linked inherent structures differ, and the associated scaling laws with the number $N$ of spins. The case of one-dimensional spin glasses is simplest and we shall use it to motivate a framework based on droplets. Such a picture predicts that the degree of the nodes in the ISN follows a Gaussian distribution with a mean growing linearly with $N$. These properties are well borne out in the one-dimensional spin glass, but when the spins lie on a random graph, fat tails appear in the distribution of the degree, indicating instead a scale-free behavior of the ISN.

The paper is organized as follows. The models are defined in Sec. II, and we also present our methods and the observables of interest. In Sec. III we investigate in detail the case of the one-dimensional spin glass. Then we present a framework based on "droplets" and give its predictions (Sec. IV); these are expected to be valid when droplets are small and "weakly interacting." Finally, in Sec. V we cover the case of spin glasses based on random graphs; there droplets are strongly interacting and context sensitive. We conclude in Sec. VI.

## II. MODELS AND METHODS

### A. Spin-glass models

We consider $N$ Ising spins lying on the vertices of a connected graph $G$ where each vertex is connected to exactly $k$ others. To each edge $ij$ of such a graph, we independently assign a weight $J_{ij}$ according to a distribution symmetrized about 0. These elements, i.e., the (random) edges and their associated weights $J_{ij}$, define the system's "quenched disorder." The energy landscape is defined from the space of spin configurations via the Hamiltonian

$$H(\{\sigma_i\}) \equiv -\sum_{\langle ij \rangle} J_{ij}\sigma_i\sigma_j, \tag{1}$$

where the sum runs over all pairs of sites connected by an edge of the graph and $\sigma_i = \pm 1$ is the Ising spin on site $i$. As in Ref. [16] the weights $J_{ij}$ are generated from a Gaussian distribution with variance

$$\mathrm{var}(J_{ij}) = \frac{J^2}{k}, \tag{2}$$

where $J$ is an energy scale set to 1 in the numerical work; this scaling allows for an extensive thermodynamic limit for all $k$, but in our case the landscape properties do not depend

 

on this rescaling. The model has an obvious global $Z(2)$ symmetry corresponding to flipping all the spins simultaneously.

We shall consider two classes for $G$. The first class is that of a one-dimensional lattice with nearest neighbors only and periodic boundary conditions ($k=2$); the simplicity of this structure allows for a relatively complete understanding of the associated ISN. The second class corresponds to 4-regular *random* graphs where each spin is coupled to exactly four other ones [17]; here a rather careful analysis is needed to compensate for the rather small sizes accessible to our numerical computations.

### B. Inherent structures and their network

There are $2^N$ possible configurations of the spins. A configuration is an *inherent structure* (IS) if and only if it is a local minimum of the energy, i.e., no single spin flip will lower the energy. (Because the $J_{ij}$ are independent and identically distributed . variables with a continuous distribution, generically the energy of an inherent structure is strictly lower than that of its neighboring configurations.)

Each spin configuration can be mapped onto a unique inherent structure using the following *steepest descent* procedure: a succession of spin flips is carried out but at each step the spin chosen for flipping is that which lowers the energy the most. The basin of attraction (hereafter simply referred to as "basin") of an inherent structure is, by definition, the set of all configurations mapped onto that structure by this steepest descent procedure.

Configuration space can be thought of as forming a Boolean hypercube: two configurations are connected by an edge if they differ by a single spin flip. Let $x$ and $y$ be two configurations mapped by steepest descent onto the inherent structures $X$ and $Y$, respectively: $x \to X$ and $y \to Y$. Suppose that $x$ and $y$ are connected by an edge (they differ by a single spin flip) and that $X \neq Y$. In this case we say that the $xy$ link crosses the frontier between the basins of $X$ and $Y$: it is a *frontier link*.

Let $xy$ be a frontier link and let $x$ be more energetic than $y$: $H(x) > H(y)$. The link $xy$ is a *transition link* if the following condition is satisfied:

$$[H(x) - H(X)] < \Lambda \quad \text{or} \quad [H(x) - H(Y)] < \Lambda, \qquad (3)$$

where $\Lambda$ is a control parameter. The situation is illustrated in Fig. 1, both for this discrete space case and for the analogous situation in a continuous space where the distinction between $x$ and $y$ is not necessary. In this figure, the configuration $x$—the more energetic vertex in a transition link—is the discrete space analog of a *transition state* (saddle) in models having a continuous configuration space (cf. [18]); the saddle in the top part of Fig. 1 is denoted by $S$. There may be many saddles between two neighboring basins, so one could think of having either multiple or weighted links between inherent structures. In the present paper we are not interested in these multiple links, but only whether there exists at least one $xy$ between given IS, which fulfills Eq. (3), in which case the two IS are connected by a link. (In this respect we follow Ref. [19].)

The ISN is defined by its nodes (the inherent structures) and its links (two nodes are linked if the corresponding inherent structures have basins connected by a transition link). It can be thought of as a directed network: by convention the direction of an edge is from the more energetic to the less energetic node. The topology of the ISN depends, of course, on the choice of $\Lambda$. For $\Lambda \ll J$ the ISN consists mostly of isolated nodes (some nodes may nevertheless be connected due to the random values of the $J_{ij}$, which occasionally make certain energy barriers small). The number of links of the ISN increases with $\Lambda$ and a giant component—defined disregarding the directionality of edges—is expected to set in when $\Lambda$ is sufficiently large.

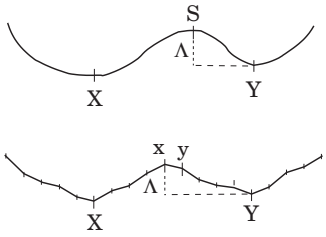


FIG. 1. Representation of an energy landscape and the associated special configurations. Horizontal axis: configuration space, vertical axis: energy. $X$ and $Y$ are inherent structures, connected by a saddle $S$ (in the continuous case, top) or by a frontier link $xy$ (in the discrete case, bottom).

### C. Algorithmic methods

Given any realization of the graph and the weights $J_{ij}$, we exhaustively consider all configurations and determine via the steepest descent algorithm the basin to which each belongs. This gives the complete map from the $2^N$ configurations to the set of inherent structures. (For computational details, see Ref. [16].) Then we determine the transition states which allow us to introduce links between inherent structures; this leads to the ISN. For all that follows, two nodes of the network are connected by at most one link of energy given by that of the lowest transition state between the two considered inherent structures. To understand the statistical behavior at large $N$ of such ISN, we repeat this construction for many disorder samples and try to extract the dependence on $N$.

The CPU time needed to execute this code for one instance of 20, 25, and 30 spins is about 2 s, 100 s, and 4000 s, respectively. It is evident that, in practice, $N \approx 30$ turns out to be a working limit for our programs. Moreover, the RAM memory demand is considerable: at $N=30$ one needs 2 Gb.

## III. ONE-DIMENSIONAL CASE

### A. Inherent structures

On the one-dimensional lattice, a configuration can be described either by the values of every spin or by the "bond" quantities $\sigma_i J_{i,i+1} \sigma_{i+1}$; these are positive for satisfied bonds and negative for unsatisfied ones. In this last representation, it is easy to give a necessary and sufficient condition for having a local minimum of the energy: each unsatisfied bond

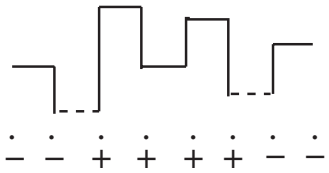

FIG. 2. Energy profile representation of configurations for the one-dimensional lattice. The dots stand for the lattice vertices, the strength of a bond is given by its "height" on the vertical axis, and the unsatisfied bonds are represented by broken segments. A particular spin configuration is indicated by the ± signs; for this configuration the second and the sixth bond are unsatisfied.

must be between two satisfied bonds, and its strength $|J_{i,i+1}|$ must be smaller than that of its neighbors.

Without loss of generality (at least if one neglects the periodic boundary conditions of the lattice), one can replace all the $J_{i,i+1}$ by $|J_{i,i+1}|$. (This follows from the gauge invariance of the Hamiltonian.) We are then led to an "energy profile" representation where each bond has a height $|J_{i,i+1}|$ and a configuration is specified by specifying which bonds are unsatisfied. In Fig. 2 we show such a representation where unsatisfied bonds are shown as broken segments, and the "height" of the bond is given on the vertical axis. Note that in ferromagnets, such unsatisfied bonds are referred to as kinks. It is straightforward to see that a configuration is a local minimum if and only if its broken segments (if any) appear only at the bottom of the profile. We shall call "elementary droplet" the region of spins contained between two successive minimum segments; a spin on a minimum segment belongs to the single elementary droplet it touches. It is easy to see that all inherent structures correspond to simply specifying the state of each elementary droplet; within the gauge where all the $J_{ij}$ are positive, each elementary droplet will have all of its spins in the +1 state or all in the −1 state.

For a given sample, let $M$ be the number of segments that are locally minimum in the energy profile. (For periodic boundary conditions, this is also the number of elementary droplets.) Then the number of inherent structures is $2^M$, a well known result [20,21]. At large $N$, $M$ is a Gaussian random variable of mean $N/3$. This follows from the fact that each segment is a local minimum with probability $1/3$. The variance of $M$ can also be calculated; the result is

$$\mathrm{var}(M) = 2N/45. \tag{4}$$

As a consequence the number of local minima $N_{IS}$, which gives the size of the ISN, is log-normally distributed for large $N$ [16] and

$$\ln\langle N_{IS}\rangle \approx \left[\frac{1}{3}\ln 2 + \frac{1}{45}(\ln 2)^2\right]N \approx 0.2417N. \tag{5}$$

### B. Transition links

Given two inherent structures $X$ and $Y$, are they linked by a transition state? This is *a priori* a difficult problem as there are many possible configurations to consider. In Fig. 3 we show how a given pair $xy$ can be visualized within the energy profile picture in a case where $Y$ is the ground state and $X$ has exactly two broken segments, $X$ and $Y$ differing by two adjacent elementary droplets.

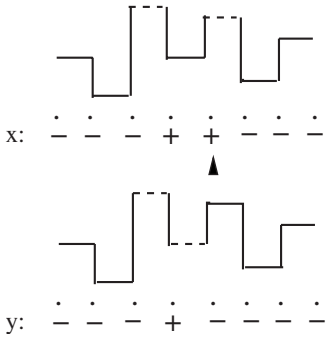


FIG. 3. Energy profile representation of a transition state $x$, and $y$ obtained by flipping the indicated spin. $Y$ here is the configuration with all bonds satisfied, while $X$, shown in Fig. 2, differs from it by a droplet consisting of two adjacent elementary droplets.

A better understanding of what links two inherent structures is achieved when one remembers a few simple facts. First, the set of unsatisfied bonds determine the system's energy: if $E_0$ is the ground-state energy where all bonds are satisfied, then a configuration's energy is given by

$$H(\{\sigma_i\}) = E_0 + 2\sum_i |J_{i,i+1}|, \tag{6}$$

where the sum runs over all unsatisfied bonds. Second, a steepest-descent path corresponds to a specific sequence of moves where at each step a single spin is flipped to lower the energy. In such downhill changes, two alternative possibilities arise. If the flipped spin belongs to two unsatisfied bonds, then these both become satisfied, a phenomenon one can refer to as "annihilation." If on the contrary the flipped spin is shared between one satisfied bond and one unsatisfied one, then the two bonds exchange their (satisfied and unsatisfied) nature. In such a move, the energy must decrease; if we think of marking broken segments on the energy profile, then the markings have to go downhill during the steepest descent. Note that when two neighboring unsatisfied bonds can annihilate one another, annihilation is always preferred to letting one of them go downhill.

In general, the linking of two inherent structures depends on $\Lambda/J$ and on the detailed values of the $J_{i,i+1}$; nevertheless some useful general properties can be derived as follows.

(i) In the energy profile picture, consider a segment $S_{i,i+1}$, which is a local *maximum*. If the corresponding bond is satisfied in both $x$ and $y$ belonging to the basin of $X$ and $Y$, respectively, then all downhill spin flips will maintain that segment's unbroken state, and thus both $X$ and $Y$ will have that bond satisfied. Thinking of this in lattice space, let $\sigma_{i_0}$ be the spin that is flipped when going from $x$ to $y$. Starting from $x$ and $y$, the steepest descent energy relaxation will produce two trajectories of configurations, whose difference (referred to as "damage" in the spin glass literature) will spread from the initiation site $\sigma_{i_0}$. The corresponding "damage spreading" [22] front going towards $i$ will stop at $i$ or before, and thus all

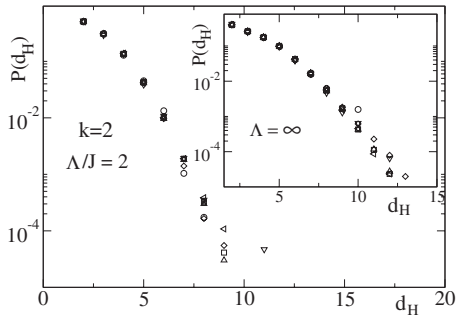


FIG. 4. Distribution of the Hamming distance $d_H$ between linked IS in the one-dimensional lattice for $\Lambda/J=2$ and for $N$ ranging from 10 to 30. The average $d_H$ is almost $N$ independent and equals 2.75(2). Inset: same but for $\Lambda=\infty$, the average $d_H$ being now 3.20(4).

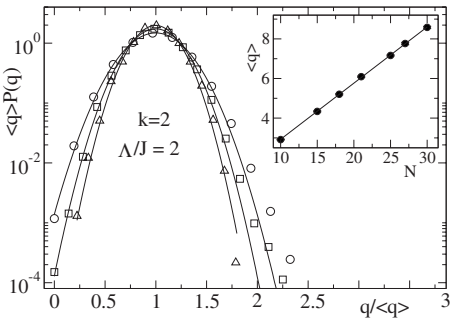


FIG. 5. Scaled distribution of degree in the ISN for the one-dimensional lattice ($\Lambda/J=2$) for $N=16$ (circles), 22 (squares), 28 (triangles) in a semilogarithmic plot. The parabola correspond to Gaussian distributions. Inset: The mean degree versus $N$, along with the corresponding linear fit $\langle q\rangle=a+bN$, where $a=0.09(3)$ and $b=0.284(1)$.

the spins beyond the "barrier" $S_{i,i+1}$ will be blind to this: the final difference between $X$ and $Y$ will vanish beyond site $i$ by "causality." In effect, information about the state of $\sigma_{i_0}$ is blocked by this barrier. This same blocking arises if the maximum segment $S_{i,i+1}$ is broken but both trajectories from $x$ and $y$ flip the same spin on that segment. (Here we use the fact that of the spins $\sigma_i$ and $\sigma_{i+1}$, one is never flipped while the other is flipped just once in the whole steepest descent; indeed, after the first flip, the bond $(i,i+1)$ is satisfied and remains so thereafter.)

(ii) Clearly, all maximum segments either start unbroken or go from broken to unbroken (and remain so) during the steepest descent moves. The previous causality argument then shows that the set of maximum segments that are affected *differently* in the two trajectories from $x$ and $y$ cannot have any gaps. Furthermore, since in $X$ and $Y$ the spins belonging to the maximum segments determine completely the spins in the corresponding elementary droplets, we see that the difference between $X$ and $Y$ must be due to the flipping of an *uninterrupted* sequence of elementary droplets.

Given this last necessary condition for inherent structures $X$ and $Y$ to be linked, one can also ask whether it is sufficient. The answer is no: empirically, it is easy to find disorder samples (values of the $J_{ij}$) for which no link will connect $X$ and $Y$ even though they differ by a connected sequence of elementary droplets. Indeed, having damage spread across a series of elementary droplets requires conditions on the successive $J_{ij}$. For example, if $J_{1,2}>J_{2,3}>\cdots>J_{m-1,m}$, then the damage spreading can propagate from site 1 to site $m$ since it does not encounter any obstacle in-between, but the probability that $m$ random numbers form such a decreasing sequence is rather small: $p(m)\sim 1/m!\sim\exp(-m\ln m)$. Given these facts, one expects a probability of propagation that decreases at least as fast as exponentially with distance. This suggests that the Hamming distances $d_H$ defined as the number of spins oriented differently in $X$'s and $Y$'s have a fast decaying distribution. This is indeed what we see in our numerical simulations, as illustrated in Fig. 4. In fact this fast decay holds for all $\Lambda$, even $\Lambda=\infty$. (Note that distances between inherent structures have also previously been considered in the context of supercooled liquids in Ref. [23] and of a one-dimensional Potts model in Ref. [24].)

### C. Degree properties of the ISN

Let us first discuss some of the topological properties of the ISN. Consider first the case $\Lambda/J$ fixed. We saw that the differences (damage) between linked IS corresponded to a connected cluster of spins formed by elementary droplets and that the corresponding distribution of $d_H$ fell sharply. For a given $X$, the number of such clusters is extensive (proportional to $N$ at large $N$) and clearly, when they are far away from one another, they are independent. Thus we expect IS to have $O(N)$ links. In the inset of Fig. 5 we show our data for the mean degree of inherent structures at $\Lambda/J=2$; the data agree very well with the linear scaling in $N$. Using the near independence of these clusters, we can also appeal to the central limit theorem. One then expects $q$, the degree of an inherent structure, to have a Gaussian distribution at large $N$. We have corroborated this property also, as illustrated in the main part of Fig. 5. Visible deviations from the Gaussian distribution occur for the small $N$ values, but go away as $N$ increases.

Now we move on to the case $\Lambda=\infty$. It is not difficult to see that for any inherent structure, a link can be formed by flipping any single one of the elementary droplets. However, it is not always possible to flip more than that, because as was mentioned before, there can arise insurmountable barriers to damage spreading; as a consequence, the number of elementary droplets that can be jointly flipped is small. These properties suggest that the degree properties of the ISN are not very sensitive to $\Lambda$ when $\Lambda$ grows as we now confirm.

Consider first the scaling of the mean degree $\langle q\rangle$. We see from the inset of Fig. 6 that indeed this quantity scales linearly with $N$, just as in the case of $\Lambda$ finite. More generally, the slope of the mean degree grows with $\Lambda$ but has a finite limit as $\Lambda\to\infty$.

Second, consider the *distribution* of the degree $q$. As shown in Fig. 6, there is a broad tail at large $q$. It turns out that the tail comes mostly from links attached to low energy states: the collective flipping of multiple elementary droplets is more likely in that situation. A subtle correlation, reflecting the shape of the energy profile, amplifies that effect: clusters of multiple elementary droplets can flip more easily when each of their constituents can flip separately.

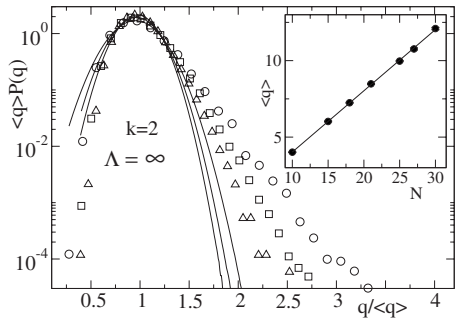


FIG. 6. Scaled distribution of degree in the ISN for the one-dimensional lattice ($\Lambda=\infty$) for $N=16$ (circles), 22 (squares), and 28 (triangles) in a semilogarithmic plot. The parabola correspond to Gaussian distributions. Inset: The mean degree versus $N$, along with the corresponding linear fit $\langle q\rangle = a + bN$, where $a=0.02(7)$, $b=0.400(3)$.

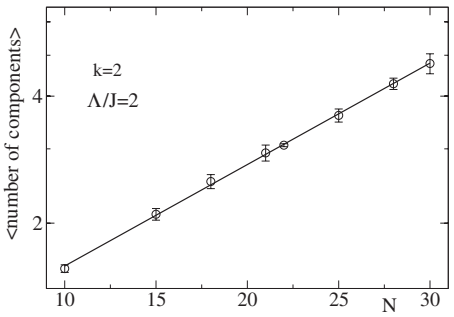


FIG. 7. Mean number of connected components of the ISN as a function of $N$ at $\Lambda/J=2.0$ for the one-dimensional lattice. Note the semilogarithmic scale indicating that the growth is exponential in $N$. [The best fit to the form $\exp(a+bN)$ gives $a=-0.09(1)$ and $b=0.0554(6)$.]

It is very significant that the tail of the distribution shrinks as $N$ increases; in particular, the effective slope in the tail gets *steeper* with $N$. Actually, it is not surprising that the deviations from Gaussian behavior are larger here than when $\Lambda$ is finite: the Hamming distances $d_H$ have a broader distribution (cf. Fig. 4). The tails in Fig. 6 arise at frequencies of $10^{-3}$ or less, and at such frequencies one has $d_H$ close to 10: to see a clear Gaussian behavior, it should be necessary to go to $N \gg 10$, and so $N=30$ can be argued to be insufficient. Given both this theoretical argument and the numerical evidence, there is some credence to the claim that the distribution becomes Gaussian at large $N$.

### D. Connected components of the ISN

When $\Lambda/J$ is finite, there may be some bonds whose state (satisfied or unsatisfied) cannot be changed during the steepest descent dynamics. Because of this, the ISN will typically consist of disconnected pieces, where in each connected component, the spins on such bonds will have fixed values.

The existence of such bonds is easily demonstrated: just consider a bond inside an elementary droplet; if its height is more than $\Lambda$ above the height of its neighbors, it must always be satisfied and thus cannot be changed. A consequence of this is that the spins inside that elementary droplet are frozen over each separate connected component of the ISN.

Let us classify each elementary droplet as being of the "frozen" type if its orientation cannot be changed when respecting the bound on energies. If elementary droplets did not touch, then the frozen nature of an elementary droplet would not depend on the state of its neighbors; in practice there is a small dependence, so for instance, an elementary droplet will be frozen in the ground state but not in some of the excited states. This *dependence on context* is weak so it is a good approximation to consider that elementary droplets are frozen or not, independently of their surroundings. An elementary droplet that is not frozen will be called "active."

Within such an "independent elementary droplets" approximation, much can be said about the topology of the ISN. If there are a total of $M$ elementary droplets and $(1-f)M$ of these are frozen, then there will be exactly $2^{(1-f)M}$ components to the ISN. (In addition, each of these components will be isomorphic.) In Fig. 7 we confirm this exponential growth in $N$ of the number of components of the ISN.

Note that the number of frozen elementary droplets is extensive in $N$, but decreases rapidly as $\Lambda$ grows. When $\Lambda \to \infty$, all elementary droplets are active and the ISN is connected. Indeed, to go from any IS to another, one can simply sequentially turn over each elementary droplet for which these IS differ: a necessary and sufficient condition to have a connected ISN is for all elementary droplets to be active.

Keeping within this approximation, we can further characterize the *structure* of each component of the ISN. Note that each of the $fM$ active elementary droplets can be separately flipped, i.e., there is one link connecting any IS to the one produced by flipping any elementary droplet; the degree of each IS will thus be at least equal to the number of active elementary droplets. If these were the only links, each component of the ISN would be a hypercube of dimension $fM$. But often, two inherent structures $X$ and $Y$ will differ by *several* consecutive elementary droplets, so each component of the ISN should be thought of as a hypercube to which additional links have been added.

A structuring of these additional links arises because the (steepest descent) dynamics occurring inside a region of active elementary droplets delimited by two frozen elementary droplets is *independent* of what happens outside of this region. Thus to construct a whole connected component of the ISN, we can first restrict ourselves to links coming from multiple elementary droplets lying within a single such delimited region.

If there are $p$ elementary droplets in a delimited region, then we focus on a reduced hypercube of dimension $p$, the vertices of which are labeled by the orientation of each of the region's elementary droplets. The vertices of this hypercube are then connected by links if and only if a corresponding transition link exists (this can be determined by finding transition states, working *solely* within the delimited region). In addition to the links between nearest neighbors on the hypercube, there can be longer range links associated with multiple elementary droplets. These connections give rise to triangles and other subgraphs that are absent in the simple picture allowing for independent two-level systems only.

Now to get a global description of the ISN, we use the fact that each IS of the full one-dimensional lattice is specified by its state in each of the delimited regions. If there are multiple such regions, then a link between two ISs occurs if and only if they are identical in all but one region and for that region a link exists as just constructed on the reduced hypercube.

## IV. GENERALIZING TO A FRAMEWORK BASED ON DROPLETS

### A. Locality and correlation volume

Elementary droplets played a central role when interpreting the ISN of the one-dimensional spin glass. In this section we show that some of the associated concepts form a natural framework for understanding what can happen in more complex models. We expose here this more general picture as well as its predictions, and then shall confront these with the actual properties of spin glasses on random graphs.

Consider $\Lambda$ given, $N$ large, and a frontier link $xy$; of the steepest descent paths from configurations $x$ and $y$, at least one is expected to be composed of $O(\Lambda/J)$ steps or less because the spin flip at each step generically leads to an $O(J)$ decrease of the energy. (In Fig. 1, it is the path from $y$ to $Y$ that is of this type since it is the one satisfying the $\Lambda$ bound.) *A priori*, it is possible that the other path is much longer since no bound on the energy applies there, but such a situation is likely to be rare for typical inherent structures. For the sake of simplicity, we shall neglect this effect and consider that both paths have $O(\Lambda/J)$ steps or less. Since the number of states accessible grows fast with energy, most of the frontier links should be close to the bound, and so one can expect to be dominated by situations in which the number of steps is indeed $O(\Lambda/J)$, rather than a much smaller number.

Given that each steepest descent path should have $O(\Lambda/J)$ spin flips, linked inherent structures will differ typically by $O(\Lambda/J)$ spin flips. Furthermore, the spins of opposite sign in those two IS cannot be too "far" away from one another on the graph $G$. The reason is causality: when flipping one spin (to go from $x$ to $y$), the subsequent steepest descent path can undergo modifications but only by propagation to nearest neighbor spins at each step. Thus for a path of $\ell$ steps, only spins within a distance $\ell$ on $G$ can be affected by choosing the starting configuration $y$ instead of $x$. This phenomenon is in direct correspondence with the standard damage spreading dynamics [22]. In the limit of a very large graph $G$ (that is, in the limit $N\to\infty$), for $\Lambda/J$ fixed, one thus expects the ISN to have links between $X$'s and $Y$'s differing in the orientation of just a few spins; furthermore these clusters should be *localized* on $G$. These properties were found to hold very nicely in the one-dimensional case, though there in addition the clusters were connected. In general there is no reason to have only connected clusters, except in the one-dimensional case where the topology is very special.

To make this picture a bit more quantitative, consider the Hamming distance $d_H$ between two linked inherent structures $X$ and $Y$. Define the mean of $d_H$ as follows:

$$v_c \equiv \langle d_H \rangle, \tag{7}$$

where the average is over linked IS and over samples. One expects $v_c$ to grow with $\Lambda/J$; the larger $\Lambda/J$ is, the further the damage spreading from frontier links can propagate. In effect, $v_c$ describes a kind of correlation volume. We saw in the one-dimensional model that $v_c$ saturates as $\Lambda\to\infty$ because of the presence of insurmountable barriers to damage spreading in that case; again this phenomenon is specific to the topology of the one-dimensional lattice. On the contrary, we shall see that $v_c$ diverges when $\Lambda$ becomes unbounded in the random graph case.

### B. Dilute droplets and scaling laws

Let $\Lambda/J$ be small and take the limit of large $N$. For each link of the ISN, we argued that the difference between the two corresponding nodes $X$ and $Y$ should come from a small localized region of spins. Let us call these "droplets" whether or not $X$ and $Y$ can be connected by a barrier less than the *current* $\Lambda/J$. For simplicity, assume that these droplets are independent; then if $M$ is the number of droplets in a sample, the number of inherent structures is $2^M$. Some of these droplets will be "active" (have a transition state satisfying the $\Lambda$ bound), others not. The fraction $f(\Lambda/J)$ of active droplets grows with $\Lambda/J$. We then see that in this picture of independent droplets, the ISN consists of a number of components that grows exponentially in $N$, just as we found for the one-dimensional model (cf. Fig. 7). In fact, taking the droplet framework literally, the ISN has $2^{(1-f)M}$ components, each of which is a hypercube of dimension $fM$; furthermore, the degree of each node in this ISN is simply $fM$.

$M$ is expected to be extensive (at least for the kinds of graphs we consider), and to have a Gaussian distribution when considering samples with different $J_{ij}$. As a consequence, the number of inherent structures should have a log-normal distribution, a property that seems to hold without restriction [16]. But our droplet framework also predicts that the *degree* of nodes in the network should have a Gaussian distribution with a mean scaling linearly with $N$; the coefficient of this linear scaling is expected to grow monotonically with $\Lambda/J$.

Of course, these predictions are based on the locality argument previously given. As $\Lambda/J$ grows, more droplets arise, their $v_c$ also grows, and so the independent (dilute) approximation may break down. Although no such breakdown occurs for the one-dimensional model, we shall see that in the case of $k=4$ regular random graphs, the system's behavior changes dramatically when $\Lambda\to\infty$.

## V. RANDOM GRAPH CASE

### A. Qualitative aspects

We now move on to the case where the spins lie on sites belonging to a connected $k$-regular random graph, one of the standard frameworks for mean-field studies of spin glasses. The connectivity property is desirable because we are limited to rather few spins; it would be unreasonable to allow our small systems to be made up of even smaller independent

subsystems. In this class of graphs, each of the $N$ sites is connected to exactly $k$ other sites, with an associated $J_{ij}$, the Hamiltonian being given by Eq. (1). We have chosen $k=4$ to have a value neither too small nor too large. Indeed, $k=3$ random graphs have a non-negligible probability of being disconnected for the $N$ values we use (the connectivity can be enforced, but it is simpler to set $k=4$; with this choice randomly generated graphs are in practice never disconnected). On the other hand, as $k$ grows, the consequences of sparseness set in at larger and larger $N$ values, and since we are limited to $N \leq 30$, it is preferable to avoid this.

These graphs have two types of quenched disorder, coming from the couplings ($J_{ij}$) and from the "geometry" (which sites are coupled to which). In comparison to the one-dimensional case, there are several very important differences associated with the graph's more complex topology. First, one cannot gauge away the signs of the $J_{ij}$ to make all couplings positive: the system is inherently frustrated. Second, one cannot introduce a local structure that will automatically block damage spreading; any obstacle can be "bypassed," a feature that (at least for nearest-neighbor interactions) has no analog in one dimension. Third, elementary droplets cannot be defined *a priori*, and no simple characterization of inherent structures allows one to enumerate them efficiently. The reason is that droplets are context sensitive. Specifically, this means that if one takes the cluster of spins defining a droplet between inherent structures $X$ and $Y$, flipping that same cluster in another inherent structure $Z$ will not in general lead to a local minimum of the Hamiltonian.

Because droplets are context sensitive, the number of inherent structures $N_{IS}$ will generally not be a power of 2. Nevertheless, one expects there will be many local excitations and this should be enough to make $N_{IS}$ have a log-normal distribution. This indeed seems to be the case as has been found before, in particular, in [16].

### B. Droplet sizes

Let us now focus on the Hamming distance $d_H$ between linked inherent structures. To begin, assume that $\Lambda$ is fixed. In the one-dimensional case, droplets were localized and connected, with $d_H$ having a distribution falling off fast at large values and almost no $N$ dependence. We show in Fig. 8 what happens in the random graph case. At the top of that figure we show the distribution when $\Lambda/J=2$, for $N$ values ranging from 10 to 30. One sees that the distribution of $d_H$ still falls off relatively fast, perhaps faster than an exponential, just as in the one-dimensional case. However, there is now a trend in $N$, the droplets typically growing when $N$ increases. In the bottom of Fig. 8 we show $v_c \equiv \langle d_H \rangle$ as a function of $N$. For $\Lambda/J=2$ the data may saturate at large $N$, but are also compatible with a logarithmic growth. [The curve on the left is $v_c=1.57(5)+0.91(2)\ln(N)$.] Since this growth could be just a finite size effect, we also show a similar plot but at a smaller value of $\Lambda/J$, viz., $\Lambda/J=0.5$. Here the saturation seems more likely: the logarithmic fit is quite poor while a fit to the form $a+b/N$ is very good. Note that random graphs naturally produce $1/N$ effects because the probability that a given site belongs to a small loop (say a triangle) is $O(1/N)$. We conclude that the observed growth is plausibly a finite-size effect although a growth continuing indefinitely at higher $N$ cannot be completely excluded.

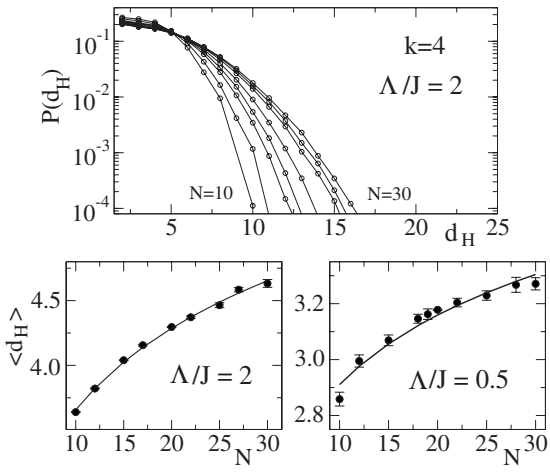


FIG. 8. Top: the distribution of the Hamming distance between linked IS for $N$ from 10 to 30 at $\Lambda/J=2$. The lines are to guide the eye. Below: The average Hamming distance versus $N$ for $\Lambda/J=2$ (left) and $\Lambda/J=0.5$ (right), along with logarithmic fits.

One might guess that the divergence of $v_c$ with $N$ depends on the value of $\Lambda$; however, our claim is that on the contrary all finite $\Lambda$ values lead to the same behavior: either $v_c$ always diverges when $N \to \infty$ or it never does. The reasoning is as follows. For specificity, take the situation illustrated in Fig. 1 where $x$ satisfies the bound with respect to $Y$. The configurations $x$ and $y$ differ from $Y$ by a finite number of spin flips. Let us assume that $v_c$ diverges so there is a nonzero probability for the damage spreading front to go arbitrarily far. In that "far away" regime, the front advances in a region of the graph $G$ where the spins are far from the few spins that are flipped to go from $Y$ to $x$. This "invasion process" will initiate with a probability that grows with $\Lambda$, but because the $J_{ij}$ are continuous and the associated local field on each spin has a finite density at 0, this initiation happens with a strictly positive probability at all $\Lambda$. The bound $\Lambda$ just plays the role of limiting the initiation probability, but does not affect the ability of the invasion process to spread arbitrarily far. Thus if $v_c$ diverges for one value of $\Lambda$, then it must diverge for all other finite values of $\Lambda$. (It may be possible to use the techniques developed in Ref. [25] to compute properties of this invasion process, at least on certain kinds of graphs.) To summarize, it seems we have just the following two alternative possibilities: (i) $v_c$ diverges with $N$, possibly logarithmically; (ii) $v_c$ saturates as $N \to \infty$. In both cases the behavior holds for all finite values of $\Lambda$.

Coming back to our data, we see that in practice damage spreading remains *relatively* localized. Note that droplets need not be connected and sometimes indeed are not, but that is rather exceptional. Comparing these results to the case of the one-dimensional spin glass, we see that the droplets are definitely larger here. Probably this has two sources: first, no single obstacle can stop damage spreading, and second, the high level of frustration in the present model should go hand in hand with enhanced fragility to perturbations. Because of

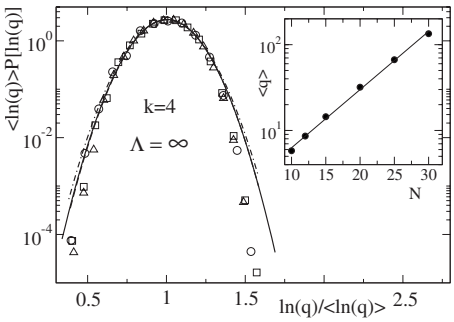


FIG. 9. Scaled degree distribution at $N=20$ (circles), 25 (squares), and 30 (triangles) for $\Lambda=\infty$. $P(\ln q)$ is normalized to unity; the bin size $\Delta \ln(q)=0.3$. The curves are obtained from log-normal fits to the data. In the inset: average degree versus $N$ [notice the logarithmic vertical scale; the best fit is $\langle q\rangle=\exp(a+bN)$, where $a=0.28(8)$ and $b=0.156(4)$].

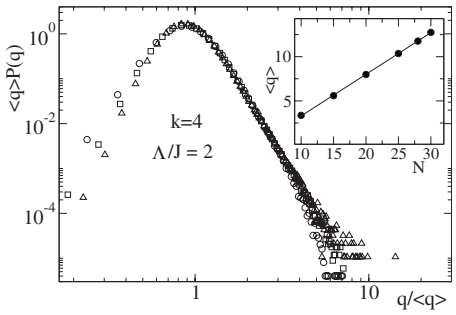


FIG. 10. Scaled degree distribution at $N=20$ (circles), 25 (squares), and 30 (triangles) for $\Lambda/J=2$. $P(q)$ is normalized to unity. In the inset: average degree versus $N$ (the best fit of the form $\langle q\rangle=a+bN$ gives $a=-1.40(6)$ and $b=0.470(3)$.

these larger droplets, one has to go to larger $N$ to hope to see the large $N$ scaling set in. In particular, for sure one needs the total number of spins $N$ to be much larger than the mean droplet volume $v_c$. However, it might be argued that it is the diameter of the graph that should be much larger than the diameter of the droplets; since the graph's diameter grows as $\ln(N)$, this would imply going to much larger values of $N$ to see the scaling set in convincingly. Such large sizes are way beyond the reach of current techniques. Note that the near logarithmic growth of $v_c$ with $N$ seen at $\Lambda=2.0$ may be related to the fact that the graph's diameter grows as $\ln(N)$, the scale where loops set in.

Finally, consider the case $\Lambda=\infty$. In the one-dimensional model, insurmountable barriers prevented $v_c$ from growing much, but here there is no reason for $v_c$ not to diverge as $\Lambda\to\infty$. Our data for $k=4$ random graphs are unambiguous here: we observe a very clean linear growth of $v_c$ with $N$, i.e., damage spreading can invade the whole system. Thus in random graph case (in contrast to what happens in one dimension), the droplet framework will be of no use for interpreting properties of the ISN when $\Lambda=\infty$: not only are droplets strongly correlated there, they are also delocalized.

### C. Degree properties at $\Lambda=\infty$

Let us first investigate the case $\Lambda=\infty$. As mentioned before, when energies are unbounded, locality no longer holds and so the droplet framework is misleading.

Consider a configuration $x$ of high energy, which under steepest descent goes to the inherent structure $X$. At high energies, damage spreading is expected to be able to propagate far away, so that $X$ should be linked to many $Y$ whose Hamming distance is proportional to $N$. Since there are no insurmountable barriers to damage spreading, the spreading can be rather sensitive to details of the configuration $x$; this picture suggests that each IS is linked to many others on the ISN, presumably an exponentially large number with $N$. This is borne out by our simulations. If $q$ is the number of links attached to $X$, we find that $\langle q\rangle$ grows exponentially with $N$ as illustrated in the inset of Fig. 9; our best fit gives

$$\langle q\rangle = e^{a+bN} \quad \text{with} \quad a=0.28(8), \quad b=0.156(4). \tag{8}$$

We know that $N_{IS}$, the number of inherent structures, is exponentially large with $N$, and here we find that $\langle q\rangle$ is also, but nevertheless the mean degree of the ISN is much smaller than the maximum possible value. Comparing with the data of Ref. [16] one finds that

$$\langle q\rangle \propto \langle N_{IS}\rangle^{\beta}, \tag{9}$$

where the exponent $\beta\approx 0.72$ is significantly less than unity.

We also mentioned that the number of IS has a log-normal distribution; the argument behind that can plausibly be applied to $q$ itself. Thus in Fig. 9 we compare the empirical distribution of $q$ to a log-normal one adjusted to have the same mean and variance. The data indicate that the distribution is steeper than log-normal, but also less steep than a Gaussian. We also find that this distribution is relatively insensitive to the $N$ values studied. But this may be misleading: if we consider the variance of $\ln q$, it increases roughly like $\langle \ln q\rangle$, though the finite-size effects are sizable. If one extrapolates the behavior of the largest system sizes accessible to us, namely, $20\le N\le 30$, one finds that the variance of the quantity $\ln q/\langle \ln q\rangle$, namely, $\mathrm{var}(\ln q)/\langle \ln q\rangle^2$ can be fit to the form

$$\frac{\mathrm{var}(\ln q)}{\langle \ln q\rangle^2} \sim \frac{a}{N}(1+b/N+\ldots), \tag{10}$$

with $b\approx -10$. This coefficient is large, making the extrapolation dangerous, but if it is correct, the distribution at large $N$ is log-normal, so the bulk of the scaled degree distribution shown in Fig. 9 will shrink, but only for $N\gg 10$.

### D. Degree properties at $\Lambda$ finite

Now we come to the case of $\Lambda$ finite, where we found droplets to be typically localized, and so the droplet framework may be expected to be a useful guide. The first prediction of the droplet framework is that $\langle q\rangle$ grows linearly with $N$. Our data are in good agreement with this scaling, and for illustrative purposes we display in the inset of Fig. 10 the linear growth of $\langle q\rangle$ with $N$ when $\Lambda/J=2$; our best linear fit leads to

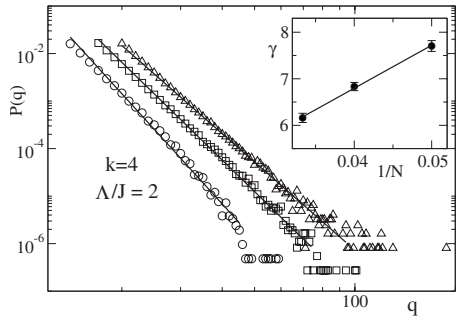


FIG. 11. Tails of the degree distributions at $N=20$ (circles), 25 (squares), and 30 (triangles) for $\Lambda/J=2$. $P(q)$ is normalized to unity. Power fits $P(q) \propto q^{-\gamma}$ are also shown. In the inset: the exponent $\gamma$ versus $1/N$; a very tentative linear fit yields $\gamma=3.1(2)+92.2(3.8)/N$ (notice that the origin of the horizontal axis is far to the left).

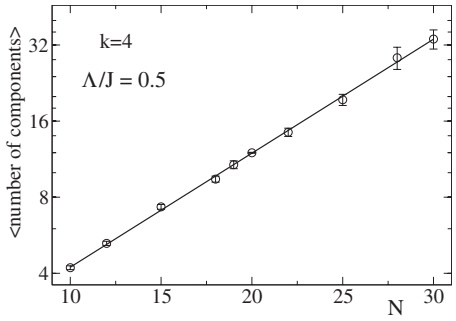


FIG. 12. Mean number of connected components of the ISN as a function of $N$ at $\Lambda/J=0.5$ for the spin glass on ($k=4$ regular) random graphs. Note the semilogarithmic scale indicating that the growth is exponential in $N$ (the best fit is $\exp[0.40(3)+0.104(2)N]$).

$$\langle q \rangle = a + bN \quad \text{with} \quad a = -1.40(6), \quad b = 0.470(3). \tag{11}$$

The second prediction of the droplet framework is that $q$ has a Gaussian limiting distribution. The main part of Fig. 10 suggests on the contrary that the distribution has a power law tail at large $q$. There is no indication that the fat tail observed is a finite $N$ effect that goes away as $N$ increases: a zoom on the tails for different $N$ shows this, as is displayed in Fig. 11. At each $N$ the tail is compatible with a pure power law; the associated exponent tends to less negative values with increasing $N$. We have performed a (tentative) $1/N$ extrapolation on the power and this works quite well (see inset), leading to the estimation of an algebraic decay with exponent $\approx 3$ in the large $N$ limit. All of these properties hold for the different values of $\Lambda$ we have investigated; in particular, the exponents of the tails are insensitive to $\Lambda$.

The behavior of the distribution is striking, because in the droplet framework the quantity $q/\langle q \rangle$ is expected to become peaked whereas we see instead a stable distribution with a fat tail. If this is indeed indicative of the large $N$ behavior, then $q$ is not self-averaging; such a situation is surprising and requires strong correlations, and presumably a diverging $v_c$. Distributions with power law tails are often called "scale-free," and many natural and artificial systems have networks with this property. Growth rules have been proposed to explain the relative ubiquity of scale-free networks [26,27], but our ISN is not the result of a growth process; thus other explanations are called for.

Just as we did for $\Lambda=\infty$, one may ask whether there is any trend that would suggest a narrowing of the distribution with increasing $N$. We have thus examined the variance of $q/\langle q \rangle$, namely, $\mathrm{var}(q)/\langle q \rangle^2$. It is possible to fit it to the form

$$\frac{\mathrm{var}(q)}{\langle q \rangle^2} \sim \frac{a'}{N}(1 + b'/N + \cdots), \tag{12}$$

with $b' \approx -10$. Again this correction term is large and compensates to a large extent the trend imposed by the first term; it also shows that a putative narrowing of the distribution can only set in for $N \gg 10$. However, in such a picture, one would still expect the amplitude of the tails in Fig. 10 to diminish with $N$, while a close observation of that figure shows that they grow slightly.

To conclude, we can interpret the data either as giving some credence to the droplet claim whereby a central limit behavior will transpire but only for much larger $N$ than we can tackle, or, more likely, as giving evidence for a limiting distribution for $q/\langle q \rangle$ at large $N$ with power law tails. In this last scenario, the system is "critical" for all finite $\Lambda$, suggesting that droplets are correlated on all scales. Since no parameter has been fine tuned, the criticality is self-organized [28].

### E. Connected components of the ISN

Just as in the one-dimensional case, it is of interest to understand the connectivity properties of the ISN. Since in the random graph case, damage spreading is less subject to bottlenecks, one expects the ISN to have fewer components than in the one-dimensional case. The greater fragility of configurations to perturbations also suggests this. Not surprisingly, our simulations confirm these expectations. For instance, when $\Lambda/J=2$, the one-dimensional case typically had multiple components, whereas in the random graph case usually there is just one component. To obtain more components, it is necessary to go to smaller values of $\Lambda/J$. In Fig. 12 we show how the mean number of components grows with $N$ for $\Lambda/J=0.5$: we find again an exponential increase, the best fit being $\exp[0.40(3)+0.104(2)N]$.

This qualitative behavior can be understood as follows. Even though there are no "topological" barriers in the spin-glass model defined on random graphs, the set of bonds whose couplings $J_{ij}$ have particularly large magnitudes can disconnect the ISN. Indeed, when $\Lambda/J$ is too small to allow for unsatisfying a bond, then that bond is frozen in an entire connected component of the ISN. The number of these frozen bonds grows extensively with $N$, and so the number of components is expected to grow exponentially with $N$. As $\Lambda/J$ grows, the number of frozen bonds drops very fast, so for relatively modest values of $\Lambda$ (given our small values of $N$) the ISN has just a single connected component.

## VI. DISCUSSION AND CONCLUSION

For studying the cooperative behavior of complex systems, it is common practice to refer to inherent structures

[1,11,29,30]. Here we took model systems based on spin-glass Hamiltonians and determined the degree and connectivity properties of the ISN, the network which interconnects the inherent structures. That network architecture is important for the system's dynamical behavior.

This kind of study has been pioneered in Refs. [12,19] in a context where the configuration space is continuous. In the models we studied here, this space (a Boolean hypercube) is discrete. Thus our first task has been to introduce an appropriate definition of the transition states, the passes between two neighboring basins of attraction of two distinct inherent structures (see Fig. 1). We found it useful to include in this definition a cutoff $\Lambda$: the energy of a transition state cannot be more than $\Lambda$ above both of its inherent structures. Of course, when $\Lambda/J$ is very small, the ISN is very weakly connected and of little interest. We have found, however, that for $\Lambda/J$ of order unity one observes in addition to the well known asymptotics for the number of inherent structures

$$\langle N_{IS} \rangle \propto e^{\alpha N}, \tag{13}$$

the following characteristic scaling behavior of the average number of transition states $N_T$:

$$\langle N_T \rangle \propto N e^{\alpha N}, \tag{14}$$

as would hold in a system regarded as a collection of equivalent and independent subsystems [5,18,31]. (Notice that this implies that the average degree of the ISN is linear in $N$.) The scaling law (14) is likely to hold in the thermodynamic limit, for any finite value of $\Lambda/J$, but we have no proof that it is indeed so. In any case, Eq. (14) suggests to interpret the data in terms of local excitations. This is the essence of our approach, our "droplets" are the local excitations of the system.

The droplet framework in its simplest version emerges naturally when the spins live on a one-dimensional lattice. In this case, for every given $\{J_{ij}\}$, the enumeration of inherent structures is particularly simple: the lattice can be unambiguously divided into nonoverlapping intervals and in each interval the spins are either all +1 or all −1 (in an appropriate gauge). Thus the inherent structure network is essentially based on independent two-level systems, the elementary "droplets" formed of connected clusters of spins.

Although the inherent structures can easily be visualized and counted for the one-dimensional spin glass, the inherent network is nevertheless nontrivial since it is not obvious at all which metastable states are connected via transition states. In the simplest case just the spins of an elementary droplet are flipped. A flip of *several* elementary droplets is also possible, under certain conditions: a necessary one is that these droplets form an uninterrupted sequence. These elementary droplets are de facto correlated, reflecting the shape of the "energy profile" of bonds: it turns out that the likelihood of a flip of a "compound" droplet made up of $n$ elementary ones is enhanced when flips of spins in "smaller" droplets made of $m<n$ elementary ones are likely. This effect produces a tail in the degree distribution. However, the topology of our one-dimensional lattice implies that the correlations effectively involve on average only a finite number of droplets. Consequently, Eq. (14) holds for all $\Lambda$. Furthermore, the degree of an ISN node is a sum of a number of independent random variables and the degree distribution tends to a Gaussian as $N \to \infty$.

The droplet framework being an excellent guide for the one-dimensional spin glass, it is natural to extend it to the more complicated mean-field spin glass defined on random graphs, although in this case the droplets are not defined without reference to the underlying inherent structures. If the one-dimensional lattice is represented by a ring, then a 4-regular graph can be regarded as a ring with multiple shortcuts; this changes the way droplets can interact and their locality is no longer evident. Furthermore, the properties of the model depend qualitatively on whether $\Lambda$ is finite or not, and in practice on the magnitude of $\Lambda$.

When $\Lambda/J \gg 1$, the scaling property, Eq. (14), no longer holds and the correlation volume (or mean droplet size) becomes comparable to the whole system. As a consequence, the droplet framework is of no use. For this strongly correlated system, instead of Eq. (14), we find that the mean degree of the ISN grows exponentially with $N$. Finally, one can argue that the degree distribution should be log-normal and this is relatively compatible with our data.

On the contrary, when $\Lambda/J$ is of order unity, the picture is closer to that of the droplet framework except that the finite-size corrections are large. In particular, most properties we find can again be interpreted in the droplet framework, with one notable exception: for $\Lambda/J$ of order unity, the degree distribution has a scale-free tail, $P(q) \propto q^{-\gamma}$ for large $q$. Moreover, and this is particularly significant, the exponent $\gamma$ *decreases* with increasing $N$. A tentative (and bold) extrapolation suggests that it might be close to 3 in the thermodynamic limit. We did not succeed to find a plausible explanation of this phenomenon. Clearly random graphs as used in mean-field spin glasses have strongly correlated droplets, allowing for collective flipping of spin clusters in the range for $N$ accessible to our study. If these correlations are so strong as to maintain a fat tail distribution in the thermodynamic limit, then clearly the droplet framework is inadequate and instead some self-organizing criticality [28] principle is at work.

Our approach differs from that used in the literature for certain atomic clusters [12,19], where the ISN structure has been interpreted using geometric arguments. We did not follow that avenue for several reasons. First, the idea that the scale-free tail of the degree distribution might reflect the properties of a dense packing of basins does not work for the system studied here: if it were true one would *a fortiori* observe this feature at $\Lambda=\infty$, when all neighbor basins are connected, but this does not happen. Second, the idea that the partition of the configuration space into attraction basins exhibits a fractal structure is untenable in our context: in our configuration space, i.e., on the Boolean cube, the number of points located at Hamming distance $r$ from a given vertex is $\binom{N}{r}$, which for $r \ll N$ equals $N^r/r!$. This shows that the space has a negative curvature; most points of a basin are located near its boundary. This is like in a symmetric Cayley tree and explains why a basin can have so huge a number of neighbors: the boundary itself is huge. Now, self-similarity in a curved space is a somewhat ill-defined concept, because the curvature sets a distance scale. Finally, we measured the ba-

sin size distribution; in contrast to the systems studied in Refs. [12,19], it *is not* scale-free.

In spite of a different way of looking at our systems, we recover several of the geometric observations made in Refs. [12,19]. The hubs of the ISN are due to low energy states; in fact often the ground state for the $N$ values we can tackle in this work. And there is a positive correlation between the degree of an ISN node and the size of the corresponding basin.

When considering the connectivity properties of ISN, we showed that for finite $\Lambda$ the number of components grew exponentially with $N$. We argued that this was necessarily the case when values of the $J_{ij}$ could be larger than $\Lambda$ since the associated bonds have to remain satisfied throughout the whole steepest descent from the transition states. Each such bond breaks the different components of the ISN into two further pieces that are of nearly identical size. As a consequence, at any fixed $\Lambda$, the largest component of the ISN represents an exponentially small fraction of the whole as $N \to \infty$: because of this there is no percolation transition. Our model can thus be contrasted with the continuous energy landscape model of Weinrib and Halperin [32]: there, by increasing the barrier value in the thermodynamic limit, a true percolation transition is found.

As already stated, we have no explanation of the appearance of the scale-free tail in the degree distribution; it remains a bit mysterious. The standard deexcitation of a metastable state occurs via a cascade of small steps connecting energetically close levels (e.g., in quantum mechanics this is due to the direct relation between transition probabilities and wave function overlaps). In a complex system like the one studied here there is a significant probability that many excited states are separated by a small energy barrier from one low energy state, which then appears to be a hub of incoming links on the ISN. Manifestly, this is not an uncommon feature, since it has been observed in a set of very different systems. One can wonder what use nature can make of this curious geometry. A clarification of this issue remains an interesting challenge.

## ACKNOWLEDGMENTS

We are very indebted to B. Waclaw for his contribution to the improvement of the efficiency of our numerical code. We also thank Satya Majumdar for helpful comments. This work was supported by the EEC's FP6 Information Society Technologies Programme under Contract No. IST-001935, EVERGROW (www.evergrow.org), by the EEC's FP6 Marie Curie RTN under Contract No. MRTN-CT-2004-005616 (ENRAGE: European Network on Random Geometry), by the Marie Curie Actions Transfer of Knowledge project "COCOS", Grant No. MTKD-CT-2004-517186 and by the Polish Ministry of Science and Information Society Technologies Grant No. 1P03B-04029 (2005-2008). The LPT and LPTMS are Unité de Recherche de l'Université Paris-Sud associées au CNRS.

[1] F. H. Stillinger and T. A. Weber, Science **225**, 983 (1984).
[2] S. Büchner and A. Heuer, Phys. Rev. E **60**, 6507 (1999).
[3] T. Bogdan, D. Wales, and F. Calvo, J. Chem. Phys. **124**, 044102 (2006).
[4] A. Crisanti, F. Ritort, A. Rocco, and M. Sellitto, J. Chem. Phys. **113**, 10615 (2000).
[5] J. P. K. Doye and D. J. Wales, J. Chem. Phys. **116**, 3777 (2002).
[6] N. Giovambattista, F. W. Starr, F. Sciortino, S. V. Buldyrev, and H. E. Stanley, Phys. Rev. E **65**, 041502 (2002).
[7] D. J. Wales and J. P. K. Doye, J. Chem. Phys. **119**, 12409 (2003).
[8] B. Doliwa and A. Heuer, Phys. Rev. E **67**, 030501(R) (2003).
[9] D. Stariolo, J. Arenzon, and G. Fabricius, Physica A **340**, 316 (2004).
[10] R. A. Denny, D. R. Reichman, and J.-P. Bouchaud, Phys. Rev. Lett. **90**, 025503 (2003).
[11] L. Angelani, G. Parisi, G. Ruocco, and G. Viliani, Phys. Rev. Lett. **81**, 4648 (1998).
[12] J. P. K. Doye, Phys. Rev. Lett. **88**, 238701 (2002).
[13] M. Mézard, G. Parisi, and M. A. Virasoro, *Spin-Glass Theory and Beyond*, Lecture Notes in Physics, Vol. 9 (World Scientific, Singapore, 1987).
[14] A. Cavagna, J. P. Garrahan, and I. Giardina, Phys. Rev. E **59**, 2808 (1999).
[15] Y. V. Fyodorov, Phys. Rev. Lett. **92**, 240601 (2004).
[16] Z. Burda, A. Krzywicki, O. C. Martin, and Z. Tabor, Phys. Rev. E **73**, 036110 (2006).
[17] C. De Dominicis and Y. Goldschmidt, J. Phys. A **22**, L775 (1989).
[18] D. Wales, *Energy Landscapes* (Cambridge University Press, Cambridge, 2003).
[19] J. P. K. Doye and C. P. Massen, Phys. Rev. E **71**, 016128 (2005).
[20] T. Li, Phys. Rev. B **24**, 6579 (1981).
[21] B. Derrida and E. Gardner, J. Phys. (Paris) **47**, 959 (1986).
[22] B. Derrida and G. Weisbuch, Europhys. Lett. **4**, 657 (1987).
[23] G. Fabricius and D. A. Stariolo, Phys. Rev. E **66**, 031501 (2002).
[24] E. Bertin, Europhys. Lett. **71**, 452 (2005).
[25] A. Montanari and G. Semerjian, J. Stat. Phys. **124**, 103 (2006).
[26] L. Barabasi and R. Albert, Science **286**, 509 (1999).
[27] P. R. Guimmaraes Jr., M. A. M. de Aguiar, J. Bascompte, P. Jordano, and S. Furtado dos Reis, Phys. Rev. E **71**, 037101 (2005).
[28] P. Bak, C. Tang, and K. Wiesenfeld, Phys. Rev. A **38**, 364 (1988).
[29] F. Sciortino, W. Kob, and P. Tartaglia, Phys. Rev. Lett. **83**, 3214 (1999).
[30] S. Sastry, Nature (London) **409**, 164 (2001).
[31] F. H. Stillinger and T. A. Weber, Phys. Rev. A **25**, 978 (1982).
[32] A. Weinrib and B. I. Halperin, Phys. Rev. B **26**, 1362 (1982).